methods

Pitfalls and solutions in assaying anandamide transport in cells[S]

Sergio Oddi,*,†,1 Filomena Fezza,†,§,1 Giuseppina Catanzaro,*,† Chiara De Simone,†,§ Mariangela Pucci,* Daniele Piomelli,,†† Alessandro Finazzi-Agrò,§ and Mauro Maccarrone[2,*,†]**

Department of Biomedical Sciences,* University of Teramo, 64100 Teramo, Italy; European Center for Brain Research/Santa Lucia Foundation,† 00143 Rome, Italy; Department of Experimental Medicine and Biochemical Sciences,§ University of Rome Tor Vergata, 00133 Rome, Italy; Department of Pharmacology,** University of California, Irvine, CA 92967; and Unit of Drug Discovery and Development,†† Italian Institute of Technology, 16163 Genoa, Italy

Abstract Nonspecific binding of anandamide to plastic exhibits many features that could be mistaken as biological processes, thereby representing an important source of conflicting data on the uptake and release of this lipophilic substance. Herein, we propose an improved method to assay anandamide transport, by using glass slides (i.e., coverslips) as physical support to grow cells. Although the results obtained using plastic do not differ significantly from those obtained using glass, the new procedure has the advantage of being faster, simpler, and more accurate. In fact, the lack of aspecific adsorption of anandamide to the glass surface yields a lower background and a higher precision and accuracy in determining transport kinetics, especially for the export process. Remarkably, the kinetic parameters of anandamide uptake obtained with the old and the new procedures may be similar or different depending on the cell type, thus demonstrating the complexity of the interference of plastic on the transport process.[JLR] In addition, the novel procedure is particularly suitable for visualization and measurement of anandamide transport in intact cells by using a biotinylated derivative in confocal fluorescence microscopy.—Oddi, S., F. Fezza, G. Catanzaro, C. De Simone, M. Pucci, D. Piomelli, A. Fizazzi-Agrò, and M. Maccarrone. **Pitfalls and solutions in assaying anandamide transport in cells.** ***J. Lipid Res.*** 51: **2435–2444.**

Supplementary key words endocannabinoids • lipid efflux • glass coverslips • plasticware • biotinylated derivative of anandamide • confocal microscopy

The endogenous cannabinoid anandamide [*N*-arachidonoylethanolamine (AEA)] carries out several biological functions, both in the central nervous system and in the periphery, by binding to type-1 and type-2 cannabinoid receptors (1), and to transient receptor potential vanilloid 1 (TRPV1) ion channels (2, 3). Additional targets of AEA also include 5-hydroxytryptamine receptors (4), GPR55 or "CB3R" (5, 6), and the nuclear peroxisome proliferator-activated receptors α (7, 8) and γ (9–11).

AEA is thought to act as an autocrine/paracrine mediator by activating these receptors either on the cell surface (cannabinoid receptors) or within the cell (TRPV1 and peroxisome proliferator-activated receptors). Extracellular AEA signaling is terminated through a two-step process consisting of transport inside the cell and subsequent hydrolysis by fatty acid amide hydrolase (FAAH) (12). The process whereby AEA is transported across the plasma membrane and within the cell is considered a hot topic, because it is a potential target for treatment of several pathologies associated with endocannabinoid system dysfunctions (13–21).

Despite considerable experimental efforts made to clarify the mechanism of AEA transport, there is not yet general consensus on the identity of the elements responsible for this process [see (22) for a very recent review]. In general, five nonmutually exclusive models have been proposed: *i*) passive diffusion (23, 24); *ii*) facilitated transport (25–27); *iii*) intracellular trafficking and sequestration (24, 27, 28); *iv*) endocytosis (29, 30); and *v*) FAAH-mediated uptake (31–33). These mechanisms might also oper-

This investigation was partly supported by the National Institutes of Health (Subaward no. 2007-1917 to M.M. under prime Grant/Contract no. 3R01DA012413-09S1 to D.P.), by Ministero dell'Istruzione, dell'Università e della Ricerca (PRIN 2008 to M.M.), and by Fondazione TERCAS (Research Program 2009-2012 to M.M.). Its contents are solely the responsibility of the authors and do not necessarily represent the official views of the National Institutes of Health or other granting agencies.

Manuscript received 18 November 2009 and in revised form 6 May 2010.

Published, JLR Papers in Press, May 6, 2010
DOI 10.1194/jlr.D004176

Abbreviations: AEA, *N*-arachidonoylethanolamine, 2-AG, 2-arachidonoylglycerol; b-AEA; biotin-AEA; CV, coefficient of variation; FAAH, fatty acid amide hydrolase; [^{3}H]AEA, arachidonoyl-5,6,8,9,11,12,14,15-[^{3}H]ethanolamine; $t_{1/2}$, half-life; TRPV1, transient receptor potential vanilloid 1, URB597; cyclohexylcarbamic acid 3′-carbamoyl-biphenyl-3-yl ester.

[1] S. Oddi and F. Fezza contributed equally to this article.

[2] To whom correspondence should be addressed.
e-mail: mmaccarrone@unite.it

[S] The online version of this article (available at http://www.jlr.org) contains supplementary data in the form of one figure.

ate simultaneously to different extents, depending on cell type and assay conditions used.

It is widely accepted that conflicting literature data on AEA transport are largely due to the methodological intricacy of measuring such a lipophilic molecule (34). In particular, the main problem might be a nonspecific adsorption of AEA onto plastic plates, resulting in a very high background noise (34). Furthermore, the adsorption of AEA to cell-free plates can be even more pronounced than that to cell-containing plates. Besides binding to the plastic in a way that can be prevented by binding inhibitors, AEA can be subsequently released in a time- and temperature-dependent manner. These features could be mistaken as biological processes, thereby representing an important source of conflicting results in both uptake and release studies (24, 35). Such concern has been addressed in a few papers that propose the use of fatty acid-free BSA in the uptake buffer to stabilize AEA solubility and to minimize its retention by plastic wells (24, 32, 34, 35). However, the use of BSA in the uptake assay has not been widely accepted, because BSA has been reported to interfere with, or even abolish, AEA uptake by cells, possibly due to the high-affinity of AEA binding to BSA (25, 36, 37).

In the present study, we sought to minimize the errors associated with the nonspecific binding of AEA to plasticware by developing a methodological alternative to traditional protocols. To this aim, we carried out the experiments on glass supports (coverslips) instead of plastic, exploiting the limited tendency of hydrophobic molecules to bind the hydrophilic surface of borosilicate glass (38). Indeed, we found that AEA does not appreciably adsorb onto the glass surface of the coverslips, thus minimizing the background noise often associated with assays performed on plastic supports. This new approach was successfully applied also to the measurement of AEA export from cells. Additionally, we demonstrated that a biotinylated derivative of AEA (b-AEA) (28, 39) can be used to visualize the in-and-out traffic of this endocannabinoid by immunofluorescence techniques, providing a nonradioactive, rapid, and easy-to-use alternative for the study of anandamide metabolism.

MATERIALS AND METHODS

Materials

All chemicals were of the purest analytical grade and were from Sigma Chemical Co. (St. Louis, MO). Arachidonoyl-5,6,8,9,11,12,14,15-[^{3}H]ethanolamine ([^{3}H]AEA, 205 Ci/mmol) was from Perkin-Elmer Life Sciences, Inc. (Boston, MA). Nonradioactive AEA was obtained from Sigma Chemical Co. Cyclohexylcarbamic acid 3′-carbamoyl-biphenyl-3-yl ester (URB597) was from Cayman Chemical (Ann Arbor, MI). OMDM-1 was purchased from Alexis (San Diego, CA). b-AEA was synthesized and characterized as described (39). Alexa Fluor 488-conjugated streptavidin and Prolong antifade kit were purchased from Molecular Probes (Eugene, OR). Round borosilicate glass coverslips (No.1; 12 mm diameter; cod. 0111520) were purchased from Marienfeld GmbH and Co. (Lauda-Königshofen, Germany). Culture media, sera, and supplements were from Euroclone (Milan, Italy).

Cell culture

Human keratinocytes (HaCaT cells) and human neuroblastoma SH-SY5Y cells were cultured as already described (40). Briefly, cells were grown in a mixture of DMEM and F12 media (1:1, v/v) supplemented with 10% fetal bovine serum, 1% nonessential amino acids, and 100 units/ml penicillin at 37°C in a 5% CO_2 humidified atmosphere. For experiments carried out with [^{3}H]AEA, cells were plated onto 24-well plates (cod. 3526; Corning Incorporated, NY) containing or not coverslips, at an initial density of 2.0×10^5 cells/well, and were incubated with supplemented medium for 18 h. For assays performed with b-AEA, 1 day before the experiment, cells were plated at 50% confluence on glass coverslips, placed into 24-well plates, and grown as described above. To increase cell attachment to the glass surface, the coverslips were coated for 2 h at room temperature with human placenta type IV collagen solution (0.1 mg/ml in 0.1 M acetic acid) and then were rinsed with sterile water (tissue culture grade) before adding cells and medium. At the beginning of each assay, the wells were washed once with 0.5 ml warm PBS. The effect of OMDM-1 on the import/export of [^{3}H]AEA or b-AEA was determined by adding this substance (50 μM) directly to the incubation medium 10 min before the experiments (28).

Methods to measure AEA transport

Assay of [^{3}H]AEA uptake in HaCaT cells with or without coverslips. The assay was based on the method described by Fowler et al. (34), adapted as described below. For dose-dependent accumulation experiments, the culture wells, containing or not round coverslips, were incubated both at 37°C and 4°C for 10 min with different concentrations of [^{3}H]AEA (200–3,000 nM) with the specific activity diluted to 50 mCi/mmol with unlabeled AEA in serum-free medium (500 μl/well). For time-dependent accumulation experiments, cells were incubated at either 37°C or 4°C for different periods of time (0–30 min range) with 400 nM AEA in serum-free medium (500 μl/well). Incubations were stopped by placing culture plates on ice and rapidly aspirating the media. The wells were then washed three times with 1 ml of ice-cold PBS containing 1% (w/v) BSA. To recover cell-associated AEA, NaOH extraction was used as described elsewhere (34, 27). In particular, cells grown on plastic were directly treated in the wells with 500 μl NaOH (0.5 M) for 15 min at 75°C, whereas cells grown on glass were first removed from the wells (using a curled needle and a pair of flat tweezers to remove the coverslips), and then they were placed in a scintillation vial and were treated with NaOH as described above. The radioactivity in these extracts was measured by liquid scintillation counting. For experiments carried out in the absence of cells, the wells, containing or not coverslips, were incubated either at 37°C or at 4°C in supplemented medium for 18 h and then AEA "uptake" was measured as described for the experiment with cells. In a preliminary set of experiments, we found that the small amounts of methanol (final concentration ≤ 0.5%) used as a vehicle for the preparation of AEA solutions did not significantly alter either cell viability or AEA transport, in keeping with previous reports (28).

Export assay with [^{3}H]AEA. To inhibit FAAH activity, 100 nM URB597 in serum-free medium was added to wells, incubated for 10 min at 37°C, then [^{3}H]AEA was added (500 μl, 400 nM with the specific activity diluted to 50 mCi/mmol with unlabeled AEA in serum-free medium) and was further incubated for 15 min at 37°C. After this incubation step, the plates were washed three times with warm PBS, and the coverslips were transferred into new multi-wells with 500 μl PBS containing 0.15% BSA and were incubated at either 37°C or 4°C. Next, the coverslips were withdrawn at different time points (0–60 min range), were placed

into scintillation vials, and radioactivity was counted as described above.

Uptake assay with b-AEA. For time-dependent accumulation, cells were incubated at either 37°C or 4°C for different periods of time (0–60 min range) with 10 μM b-AEA in serum-free medium (0.25 ml/well). Because b-AEA is not hydrolyzed by FAAH (28), the addition of URB597 in the culture medium was omitted. For concentration-dependent accumulation experiments, cells were incubated at either 37°C or 4°C with b-AEA in the 0–20 μM range. After incubation, the plates were placed on ice and the wells were rinsed three times with ice-cold PBS. The coverslips were then transferred into new multi-wells containing 0.3 ml of fixative solution [PBS containing 3% (w/v) paraformaldehyde and 4% (w/v) sucrose] for 20 min at room temperature. Cells were extensively washed with PBS, and the excess of fixative was removed by incubating cells for 5 min at room temperature with PBS + 0.2 M glycine. After fixation, b-AEA was revealed by incubating the coverslips with the streptavidin Alexa Fluor 488-conjugated, diluted 1:100 in PBS + 0.05% saponin for 30 min at room temperature. After three washes with PBS + 0.001% saponin, coverslips were almost air-dried, mounted with 4 μl of ProLong Gold antifade, and analyzed by a Leica TCS SP confocal microscope equipped with a 40× oil objective (Leica Microsystems, Wetzlar, Germany). Pictures were taken using the program LAS AF (Leica Microsystems) and then were processed with Adobe Photoshop CS2 (Mountain View, CA) for adjustments of brightness and contrast. For image analysis, five fields from at least three independent experiments were examined for each treatment. Quantification of the mean fluorescence intensity in selected regions was carried out using the ImageJ software (http://rsb.info.nih.gov/ij/).

Export assay with b-AEA. A preloading step was carried out by incubating cells with 10 μM b-AEA in serum-free medium for 10 min at 37°C. Because b-AEA is not hydrolyzed by FAAH (28), the addition of URB597 in the culture medium was omitted. After incubation, the plates were washed three times with warm PBS. The coverslips were then transferred into new culture wells containing 500 μl serum-free medium with 0.15% BSA and were incubated at either 37°C or 4°C. The coverslips were withdrawn at different time points (0–60 min range), washed once with 0.5 ml ice-cold PBS, transferred into new wells containing 0.3 ml of fixative solution, and labeled with streptavidin-488 for fluorescence detection as described above.

Statistical analysis

Data reported in this paper are the means ± SD or ± SEM (as indicated) of at least three independent experiments, each performed in triplicate. Statistical analysis was performed by using unpaired Student's *t*-test, elaborating experimental data by means of Prism 4 program (GraphPAD Software, San Diego, CA).

RESULTS

Interaction of AEA with plastic and glass supports

As an initial experiment aimed at evaluating the different adsorption of [^{3}H]AEA on plastic or glass, plastic plates as such were incubated for 10 min either at 37°C or at 4°C with increasing concentrations of [^{3}H]AEA in buffer in the presence or absence of coverslips. As shown in **Fig. 1**, strong nonspecific AEA adsorption on plastic was observed that was both concentration- and temperature-dependent. Moreover, the temperature-sensitive component of this binding, obtained by subtracting the uptake at 37°C from that at 4°C, was better fitted to a rectangular hyperbola (dotted line in Fig. 1; R^2= 0.945) than to a straight line (R^2= 0.842), yielding apparent K_m and V_{max} values of 0.84 ± 0.25 μM and 0.34 ± 0.01 pmol AEA/min/cm^2, respectively. These data indicate that the binding of AEA to polystyrene is indeed a high-capacity, low-affinity process that mimics a protein-mediated binding (41). In marked contrast, neither a concentration- nor a temperature-dependent retention of tritium-labeled AEA was found on the coverslips, demonstrating that AEA does not bind appreciably onto glass surfaces (inset to Fig. 1). In particular, by recovering the total amount of AEA adsorbed on the two types of support, we could estimate that plastic binds AEA ∼80-fold more avidly than glass. We also checked that precoating the coverslips with collagen did not affect the binding of AEA to these glass supports (see supplementary data). Incidentally, similar results were also obtained for 2-arachidonoylglycerol (2-AG), another major endocannabinoid. In keeping with its lipophilic nature [logP = 5.39 (16)], we found that 2-AG binds to plastic to the same extent as AEA, and indeed ∼8% of total 2-AG was bound aspecifically to plastic, while only ∼0.1% was bound aspecifically to glass. Therefore, glass should also be preferred for the study of 2-AG transport. However, in the present study, we further characterized the coverslip-based procedure only for AEA transport, because we planned to use it with b-AEA, which is not yet available for 2-AG.

AEA uptake in HaCaT cells: plastic versus glass substrate

Next, the nonspecific binding of AEA to plastic and glass supports was compared with the specific uptake of AEA by cells cultured on plastic wells or coverslips. For these assays, we used HaCaT cells, a human keratinocyte cell line with a well-defined AEA transport (28, 40, 42). HaCaT cells adhere strongly to both plastic and glass supports, thus minimizing problems of cell detachment during processing and washing. The results are shown in **Fig. 2A**. Using the plastic substrate, we found that both at 37°C and 4°C the level of binding of AEA to plates with cells was ∼5-fold greater than that associated to plates alone, whereas the temperature-dependent component of cellular uptake was only ∼3-fold higher. On the contrary, when the assay was carried out with glass coverslips, the radioactivity recovered was due exclusively to AEA taken up by cells, because the uptake by the naked coverslips was negligible (i.e., from ∼30- to ∼60-fold lower than in the presence of cells). Importantly, these results showed that subtracting the uptake at 4°C from that at 37°C was not sufficient to eliminate the nonspecific signal, because a significant difference (P< 0.01) was observed between the 37°C − 4°C value of the conventional method and that of the new procedure (0.90 ± 0.08 vs. 0.56 ± 0.01 pmol/min/cm^2, respectively). Therefore, a conventional AEA uptake experiment should be carried out with cells in plastic wells at 37°C and 4°C, as well as in cell-free plastic wells. In fact, the total AEA uptake obtained by subtracting the 37°C − 4°C value of plastic without cells from the same value of plastic with cells was identical to the 37°C − 4°C

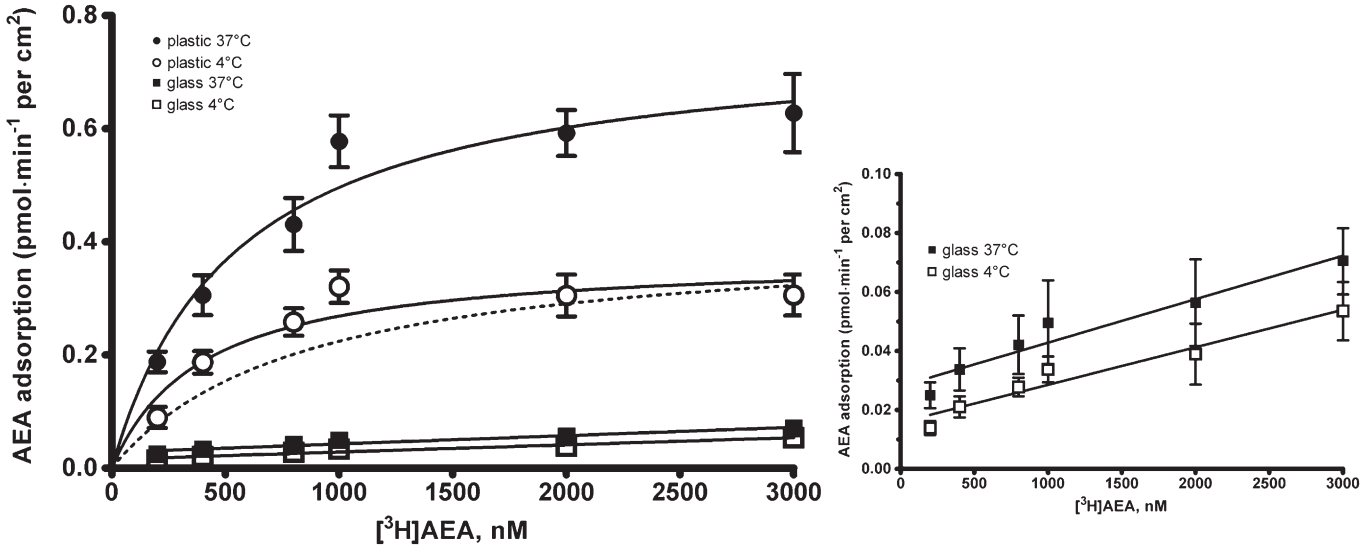

Fig. 1. Interaction of AEA with plastic and glass supports. Plastic culture wells without cells were incubated for 10 min with increasing concentrations of [^{3}H]AEA, alone [plastic, at 37°C (closed circle), or at 4°C (open circle)], or in the presence of coverslips [glass, at 37°C (closed square) or at 4°C (open square)]. The accumulation was stopped by buffer removal, and the amount of tritium adsorbed nonspecifically to the different supports was measured after washing. To compare AEA adsorption on coverslips and plastic wells, the total amount of AEA was normalized to the total wet surface of the two types of support and was expressed as pmol/min/cm^2. The temperature-sensitive component of the nonspecific uptake associated to the plastic wells was obtained by subtracting the uptake at 37°C from that at 4°C, and is shown as dotted line. The inset (on the right) shows an enlargement of the graph relative to [^{3}H]AEA retained by the coverslips. Values are means ± SEM of at least three independent experiments performed in triplicate. The points were generated using GraphPad Prism, and the curves were fitted using the one site binding hyperbola.

value obtained by using glass with cells. Taken together, these results demonstrated that, in order to calculate the specific uptake of AEA, with the conventional procedure it is necessary to perform additional controls (i.e., uptake experiments in cell-free plastic wells at 37°C and 4°C), whereas with the novel procedure these controls are not necessary.

Under the same conditions, when the experiments were carried out in the presence of various amounts of albumin in the assay buffer, we observed ~80% (at 1% BSA) or ~100% (at 5% BSA) inhibition of AEA internalization (supplementary Fig. I). Therefore, all subsequent uptake assays were performed without BSA.

To validate the new procedure, a comparison with the conventional method was made by measuring AEA uptake in HaCaT cells grown on coverslips or plastic wells (Fig. 2B; **Table 1**). Kinetic analysis of the data revealed a significant difference in the K_m constant, which was ~40% smaller when measured with the new procedure [K_m (μM): plastic, 0.47 ± 0.15, coefficient of variation (CV) = 31%; glass, 0.27 ± 0.05, CV = 19%; $P < 0.01$, n = 9]. Instead, no significant difference was observed in V_{max} values (in pmol/min/mg of protein): plastic, 125 ± 15, CV = 12%; glass, 130 ± 1, CV = 0.8%. It is noteworthy that the experimental data obtained with the new method were more regularly distributed along a rectangular hyperbola (R^2 = 0.999) compared with those obtained with the conventional procedure (R^2 = 0.910), as suggested also by the smaller CV of the estimated parameters. Moreover, the measurements made with the new protocol showed a relative error not exceeding 3% compared with ~10% of the conventional method, thereby indicating that the former procedure was more precise.

The two procedures were also compared in terms of the time dependence of [^{3}H]AEA accumulation. To this end, HaCaT cells were incubated with 400 nM AEA at various time points. Importantly, we measured AEA uptake by holding the coverslips with a pair of tweezers in the import/export buffer and then transferring them in the washing buffer to stop the reaction. By using this approach, we managed to analyze time points as early as 3 s, 15 s, and 30 s. Kinetic analysis of these data revealed a significant difference in the $t_{1/2}$ values of the process that was ~2-fold smaller when measured with the new procedure [$t_{1/2}$ (min): plastic, 5.1 ± 2.7, CV = 52%; glass, 2.5 ± 0.7, CV = 28%; $P < 0.05$, n = 9] (Fig. 2C; Table 1).

Finally, as a further control of the validity of the new procedure, we treated cells grown on coverslips with OMDM-1, a widely used inhibitor of AEA transport (37). As expected, when cells cultured on glass coverslips were preincubated with OMDM-1, both dose-dependent and time-dependent uptake of AEA was significantly reduced (Fig. 2B, C).

Export assay of [^{3}H]AEA in HaCaT cells grown on coverslips

The release of adsorbed AEA from the plastic wells could represent a major source of errors in release experiments, because it mimics a genuine biological process (35). Thus, we have explored the suitability of the new procedure to characterize the efflux of AEA from preloaded cells. Coverslips in the presence or absence of cells were incubated in 24-well plates for 10 min with 400 nM [^{3}H]AEA in the presence of 100 nM URB597, a FAAH inhibitor that minimizes AEA catabolism (17). After washing

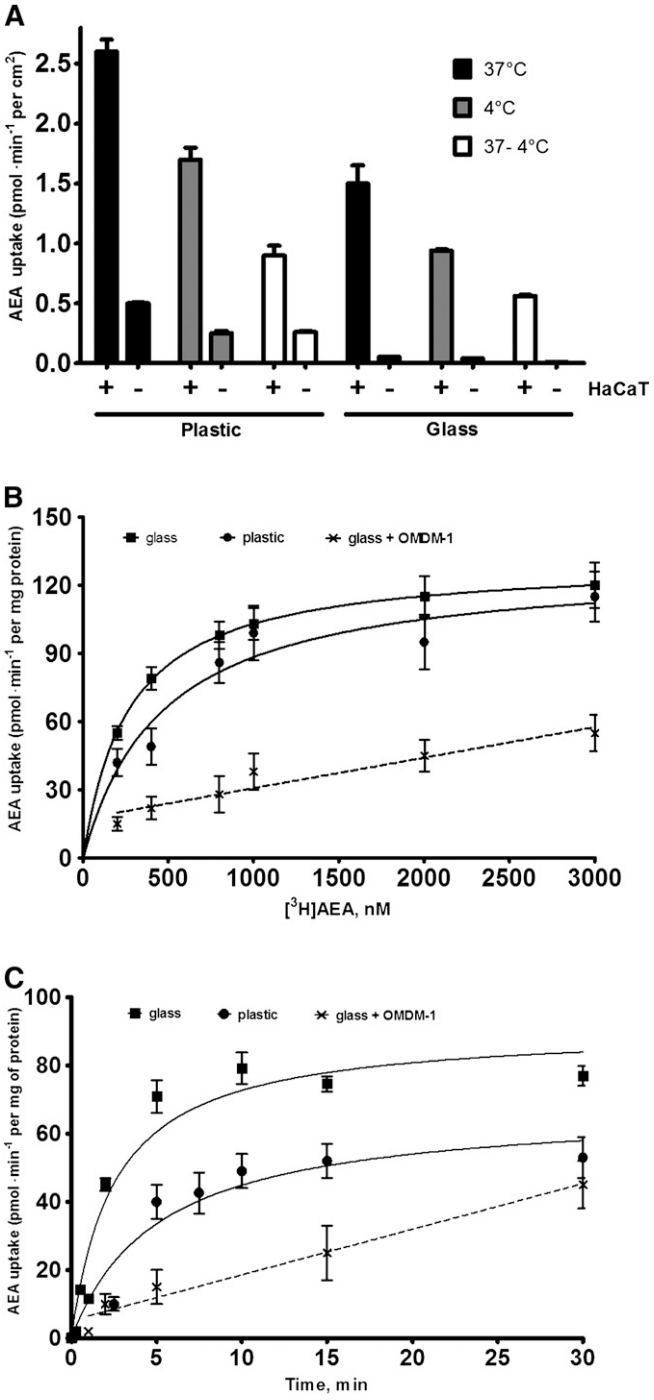

Fig. 2. Binding of AEA to plastic or glass supports in the presence or absence of cells. A: Cells or supports alone were incubated for 10 min with 400 nM [^{3}H]AEA in cell culture media. The uptakes (means ± SEM, n = 9) at 37°C (black columns), 4°C (gray columns), and 37°C − 4°C (unfilled columns) are shown, each measured in the presence (+) or absence (−) of HaCaT cells. The rate of uptake was related to the total surface in contact with AEA solution, thus allowing the comparison of uptake values among different conditions. B: Concentration dependence of [^{3}H]AEA uptake by HaCaT cells. These cells were grown onto plastic wells (closed circle) or coverslips (closed square) and were incubated with varying concentrations of AEA for 15 min at 37°C. C:Time-dependent uptake of [^{3}H]AEA in HaCaT cells. Cells were grown onto plastic wells (closed circle) or coverslips (closed square) and were incubated with 400 nM AEA at 37°C for the indicated periods of time, then they were washed and radioactivity was evaluated as described in "Materials and Methods." Inhibitory effects of 50 μM OMDM-1 (×) on both concentration- and time-dependent [^{3}H]AEA uptake were evaluated in cells grown onto coverslips. Nonspecific adsorption of AEA to cell membranes or cell supports was estimated by running the identical experiments at 4°C and was subtracted from each data point. The lines drawn are the best fit of the data to the one site binding hyperbola. Values are means ± SEM of at least three independent experiments, each performed in triplicate.

the wells to remove the unbound [^{3}H]AEA, the coverslips were transferred into new plastic wells to avoid possible contamination due to the release of AEA by the plastic. Buffer containing 0.15% BSA was then added, and the residual radioactivity of the cells or the coverslips was followed over time. As expected, in the absence of cells, neither time- nor temperature-dependent release of tritium was found at temperatures of 37°C and 4°C (data not shown); yet, in the presence of cells, a $t_{1/2}$ value of 2.4 ± 0.8 min could be calculated by fitting the temperature-dependent component of the AEA efflux with a first-order equation (**Fig. 3**).

Fluorescence-based method for the study of AEA import/export

Although both methods are able to quantify AEA import and export, they do not allow to "see" the movement of this lipid. In previous studies (28, 39), we reported the synthesis and characterization of a biotinylated analog of AEA, b-AEA, that is transported like AEA, making possible the visualization of this process. To test whether b-AEA may also represent an alternative tool for measuring the in-and-out transport of AEA by intact cells, we analyzed kinetics of b-AEA transport using fluorescence detection of cells grown onto coverslips. Preliminarily, we tested whether b-AEA was binding to glass surface alone, and found that it did not, much like AEA (data not shown). Kinetic analyses of the fluorescence values showed that the uptake of b-AEA was a saturable process with an apparent K_m of 5.8 ± 1.3 μM (**Fig. 4A**). The time dependence of b-AEA accumulation was also investigated by incubating HaCaT cells with 10 μM b-AEA at various time points. Kinetic analysis of the fluorescence values revealed that the uptake of b-AEA was time dependent, with a $t_{1/2}$ of 5.4 ± 1.0 min (Fig. 4B). Much like AEA transport, both concentration- and time-dependent uptake of b-AEA was strongly reduced by OMDM-1 (Fig. 4A, B).

Afterwards, to characterize the suitability of b-AEA as an immunofluorescence-detectable probe in export assays, we investigated the efflux of this substance from the cells. As described above for the AEA export assay, coverslips in the presence or absence of cells were preloaded with 10 μM b-AEA in 24-well plates for 30 min at 37°C. Then the coverslips were transferred to new 24-well plates and incubated for the indicated times before being fixed and analyzed by fluorescence microscopy. When the assay was performed in the absence of BSA, a slow efflux of AEA was observed with a $t_{1/2}$ of 22 ± 5 min. In contrast, the presence of 0.15% BSA in the incubation medium determined a net

TABLE 1. Comparison of the kinetic parameters of AEA transport obtained by the two procedures in human HaCaT cells and SH-SY5Y cells

	Import						Export	
	K_m (μM)		V_{max} [pmol/(min·mg)]		$t_{1/2}$ (min)		$t_{1/2}$ (min)	
Cell Line	Plastic	Glass	Plastic	Glass	Plastic	Glass	Plastic	Glass
HaCaT	0.47 ± 0.15	0.27 ± 0.05**	125 ± 15	130 ± 1	5.1 ± 2.7	2.5 ± 0.7*		2.4 ± 0.8
SH-SY5Y	0.49 ± 0.23	0.46 ± 0.12	41.5 ± 5.2	16.2 ± 1.9***				1.1 ± 0.2

Data are means ± SD values, n = 9 for each value. * Indicates $P < 0.05$ versus plastic control; ** indicates $P < 0.01$ versus plastic control; *** indicates $P < 0.001$ versus plastic control.

efflux of b-AEA that was greater at 37°C than at 4°C (Fig. 4C). The temperature-dependent component of the b-AEA efflux, calculated as the 37°C − 4°C difference, followed first-order kinetics with a $t_{1/2}$ value of 5.6 ± 1.5 min (Fig. 4C, filled squares). Finally, we found that the addition of 50 μM OMDM-1 caused a small yet not significant reduction in the efflux of b-AEA from the cells (Fig. 4C).

Experiments with SH-SY5Y cells

To further extend the analysis, a comparison of the kinetic parameters of AEA transport obtained by the old and the new procedure was carried out using a different cell line, namely human neuroblastoma SH-SY5Y cells (Table 1). At variance with the data obtained with HaCaT cells, the two procedures yielded different V_{max} values but similar K_m values for AEA uptake (Table 1), suggesting a different interference of plastic in SH-SY5Y cells. Concerning the export process, neuroblastoma cells were found to release AEA with a $t_{1/2}$ value of 1.1 ± 0.2 min, i.e., ~2-fold faster than HaCaT cells. Finally, the kinetic parameters of b-AEA transport in SH-SY5Y cells were in the same order of magnitude as the values found in HaCaT cells (**Table 2**).

DISCUSSION

An accurate estimate of uptake and release of AEA by cultured cells is a prerequisite for identifying the mechanism of AEA transport. Unfortunately, these measurements are spoiled by the tendency of AEA to adsorb reversibly not only to the plasma membranes, but also to the plastic of the culture wells, resulting in a high background noise (24). The poor signal-to-noise ratio associated with AEA uptake assays may generate artifacts that complicate the interpretation of the data, masking the effective nature of the transport process (34, 43, 44). Running identical experiments in parallel where cells are incubated at 4°C (25), or in the presence of an excess of unlabeled AEA (25) or of the AEA uptake inhibitor AM404 (45), are among the tricks used so far to determine the extent of nonspecific signals. Another system for the evaluation of nonspecific binding of AEA to cell membranes and culture dishes is the use of plates without cells or with cells incubated for only 3 s at 37°C (31–33). A further method is based on the use of BSA as AEA-binding agent, which keeps AEA in solution and prevents its adsorption to the plastic surface (24, 32). However, these methods are all subjected to various degrees of uncertainty and misinterpretation, as it has been extensively reviewed elsewhere (43, 44). Thus, development of new techniques that could overcome these shortcomings and allow a more reliable analysis of AEA transport are needed.

Here, we describe an improvement of traditional protocols aimed at minimizing the spurious phenomena affecting the accuracy of AEA transport assays. Our method simply replaces plastic wells with coverslips in uptake experiments, thus exploiting the low adherence of AEA to the borosilicate surface. Indeed, we found that the "specific uptake" of AEA measured with the standard procedure (i.e., with cells grown onto plastic), normally obtained by subtracting the uptake at 37°C from that at 4°C, was significantly higher than the corresponding value measured with the new procedure, indicating that the "standard" controls currently used to correct for the nonspecific AEA uptake are not completely reliable. In fact, we found that, in order to obtain a more accurate estimate of AEA uptake with the conventional protocol, it is necessary to perform additional controls (i.e., uptake experiments in cell-free plastic wells at 37°C and 4°C). Incidentally, the same advantages of the new protocol seem to hold true also for the transport assay of 2-AG,

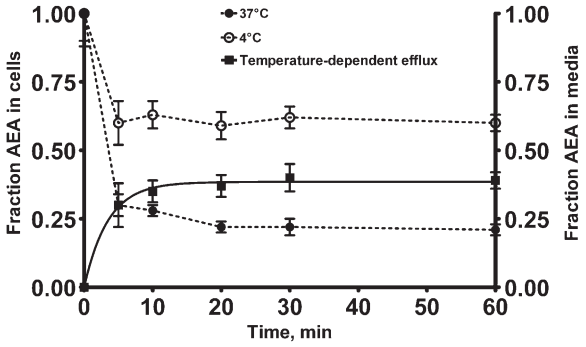

Fig. 3. Time- and temperature-dependent release of [^{3}H]AEA from HaCaT cells grown on coverslips. HaCaT cells were preloaded with 400 nM [^{3}H]AEA for 10 min at 37°C. Fresh buffer was added and the cells were incubated at either 4°C (open circle) or 37°C (closed circle) for the indicated time periods. Release was measured by extracting [^{3}H]AEA retained onto coverslips with NaOH. The temperature-dependent efflux (closed square) was calculated by subtracting the fraction of [^{3}H]AEA remaining within the cells at 37°C from the fraction remaining at 4°C. The line drawn through the filled squares is the best fit of the data to the one phase exponential association using least squares, nonlinear regression analysis (GraphPad Prism). Values are means ± SEM of at least three independent experiments performed in triplicate.

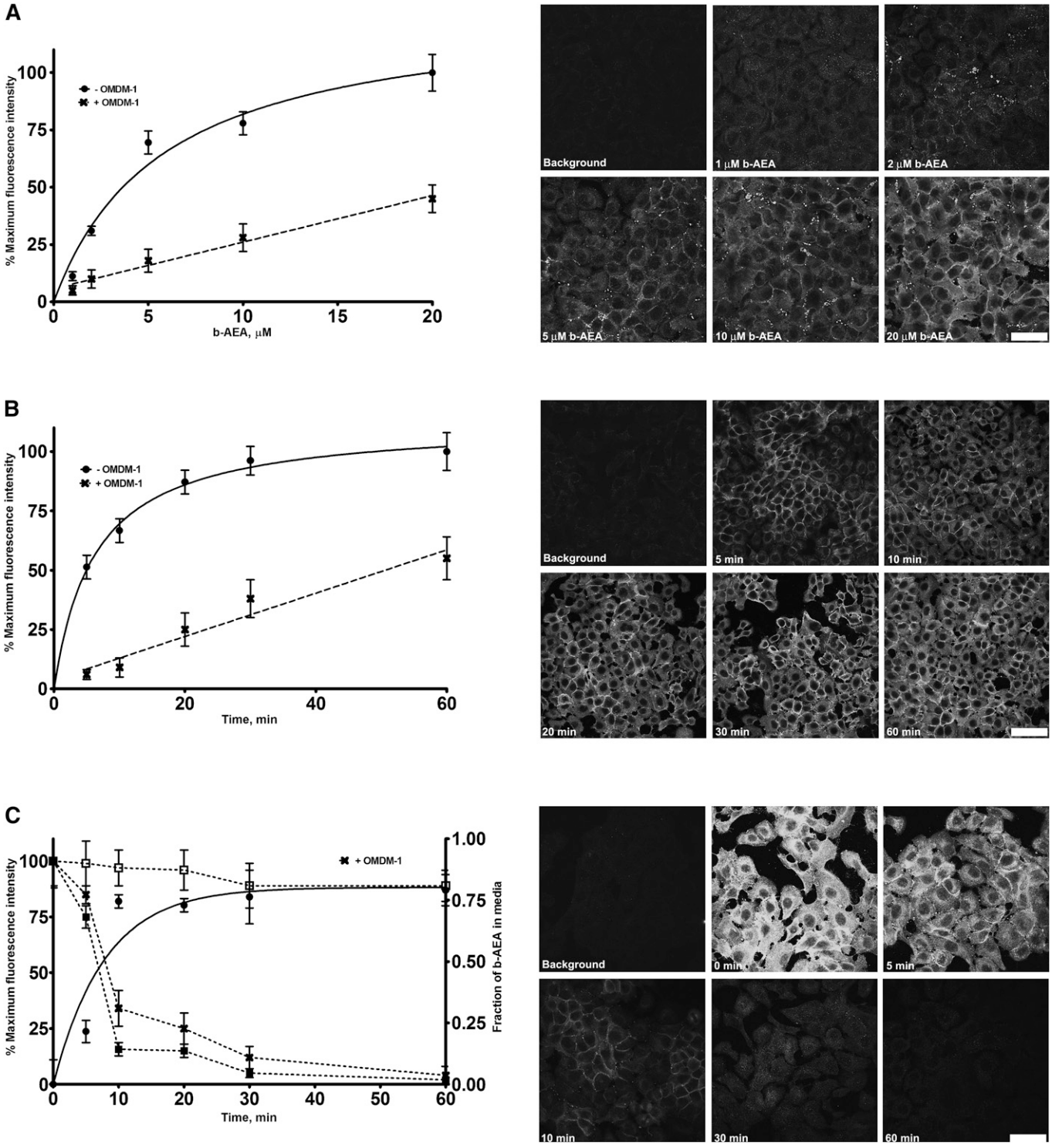

Fig. 4. Kinetics of accumulation and release of b-AEA in HaCaT cells grown onto coverslips. A: Concentration-dependent accumulation of b-AEA. HaCaT cells were incubated with the indicated concentrations of b-AEA for 10 min at 37°C, then cells were washed and subjected to microscopy detection. B: Time-dependent accumulation of b-AEA. HaCaT cells were incubated with 10 μM b-AEA at 37°C for the indicated time periods, then cells were washed and subjected to immunodetection. C: Time-dependent release of b-AEA. HaCaT cells were preloaded with 10 μM b-AEA at 37°C for 30 min, then were placed in fresh incubation medium (containing 0.15% BSA) at 37°C (closed square) or at 4°C (open square). At the indicated time points, cells were washed, fixed, and analyzed by immunofluorescence. The temperature-dependent release (closed circle) was calculated by subtracting the fraction of [^{3}H]AEA remaining within the cells at 37°C from the fraction remaining at 4°C. Inhibitory effects of 50 μM OMDM-1 (×) on both import and export of b-AEA were also evaluated. Plotted data represent the mean ± SEM fluorescence intensity measured in five fields of three independent experiments. Representative images coming from b-AEA immunostainings are shown on the right side of each graphs. Scale bars, 50 μm. Fluorescence intensity was quantified by the ImageJ software. The points were generated using GraphPad Prism, and the curves were fitted using the one site binding hyperbola for accumulation data and the one phase exponential association for release data.

TABLE 2. Kinetic parameters of b-AEA transport in human HaCaT cells and SH-SY5Y cells

	Import		Export
Cell Line	K_m (μM)	$t_{1/2}$ (min)	$t_{1/2}$ (min)
HaCaT	5.8 ± 1.3	5.4 ± 0.7	5.6 ± 1.5
SH-SY5Y	10 ± 2	3.1 ± 0.1	4.6 ± 0.6

Data are means ± SD values, n = 9 for each value.

which sticks to plastic as much as does AEA; thus, glass may be preferred over plastic to study the uptake of this endocannabinoid.

On the other hand, comparison of the kinetic parameters of AEA transport obtained by the old and the new procedure in two different cell lines (HaCaT and SH-SY5Y) demonstrated that plastic may have a significant influence on either K_m (HaCaT) or V_{max} (SH-SY5Y) values (Table 1) and possibly on both parameters in yet other cell types. The most likely explanation for these findings is that AEA binding to polystyrene is a high-capacity, low-affinity process that mimics a protein-mediated binding with typical K_m and V_{max} values. Therefore, plastic binding may contribute to different extents to the overall uptake, based on the ratio between the surface covered by cells and the surface that remains cell-free. In other words, it is likely that the degree of "uptake" contributed by the plastic depends on the cell density, because only the surface of the well directly in contact with the substrate solution (i.e., not covered by the cells), may adsorb AEA (24, 41). In this context, it is noteworthy that the two cell types used in this study have very different phenotypes, and thus, even at a 100% confluence, they occupy a different fraction of the available surface: keratinocytes cover almost completely the area of the plastic well, whereas neuroblastoma cells occupy only part of it. More generally, other variables such as incubation time, temperature, batch of culture wells, and number of cell passage may contribute to the extent of AEA adsorption to plastic, which has been reported to vary from ~5% (46) to as much as ~50% (47) of the total amount taken up. Thus, an important advantage of substituting plastic with glass is the possibility to minimize these sources of variability in the in/out transport assays.

Another major finding of this investigation is that the use of coverslips as cell support eliminates the problem of the release of adsorbed AEA from plastic wells, a major source of error in release experiments (35). Indeed, in the absence of cells, we did not observe any release of [^{3}H]AEA from the coverslips, whereas preloaded cells grown on glass displayed a well-defined time- and temperature-dependent efflux of tritium, with a temperature-dependent component following a first-order kinetics ($t_{1/2}$ = 2.4 ± 0.8 min and 1.1 ± 0.2 min for HaCaT and SH-SY5Y, respectively). Incidentally, these values are very similar to those previously observed for other cells, like cerebellar granule cells ($t_{1/2}$ = 1.9 ± 1.0 min) (25), HUVEC endothelial cells ($t_{1/2}$ = 5.0 ± 1.0 min) (48), and C6 glioma cells ($t_{1/2}$ = 3.4 ± 1.0 min) (35), overall suggesting that the efflux of AEA from the cells is indeed a rapid and efficient process.

Finally, we took advantage of the glass support to develop a fluorescence-based method for studying import and export of AEA by confocal microscopy, using a biotinylated analog of AEA (b-AEA). This substance provides a nonradioactive tool for visualizing the movement of this lipid in intact cells (28, 39). The time-dependent accumulation assay showed that the uptake of b-AEA in both cell types occurred within minutes (Table 2). Interestingly, the temperature-dependent component of b-AEA efflux from the same cells, calculated by subtracting the values at 37°C from those at 4°C, followed a first order kinetics with $t_{1/2}$ values very close to the values of the import process (Table 2). On this basis, it can be suggested that a common transport mechanism underlies the bi-directional flux of AEA across the plasma membrane (25, 27, 37, 48). However, the fact that OMDM-1 reduced the import but not the export of b-AEA in HaCaT cells seems to favor the hypothesis that these two processes are not identical.

Other critical methodological concerns about AEA uptake assays are still open, including: *i*) the optimal delivery of AEA to the cells, which can occur with or without albumin in the buffer; *ii*) the determination of the activity of AEA in aqueous solutions; and *iii*) the choice of the incubation times, which could highlight different events involved in the intracellular transport of AEA (i.e., transmembrane transport, intracellular accumulation, and subsequent metabolism). In the present study, albumin was not included in the buffer, because we observed a marked reduction of uptake both for AEA and b-AEA; instead, it was added in the export buffer, because no appreciable efflux of AEA or b-AEA could be measured in its absence. These results are comparable to those reported in previous studies (25, 35, 36), although they are in conflict with others (24, 32), overall calling for a standardization of the current protocols. With respect to the timing of the import/export assays, we used late time points (15 min for the uptake, and 5–60 min for the export), common to most transport protocols currently employed. Yet, it should be stressed that the assay with the coverslips is suitable to assess AEA import/export also at early time points (even 3 s). In fact, washing and recovering the cells after incubation can be faster than with the classical procedure, due to the possibility of holding the coverslips with a pair of tweezers in the import/export buffer and then of transferring them in the washing buffer to stop the reaction.

From a practical point of view, there are several reasons to favor the use of coverlips for assaying the transport of AEA and, potentially, of 2-AG and other endocannabinoids. First, by reducing the number of controls, the costs of each assay can be reduced by ~50% compared with the classical method. Also, the low cost of the coverslips (only $90 for 700 pieces), compared with that of plasticware for cell culture, contributes to save money. Second, growing cells on the coverslips allows to save time during the harvesting step. In fact, by rapidly moving the coverslips directly into the scintillation vials, it is possible to avoid the boring and time-consuming step of scraping cells off the plastic well. Third, if this procedure is applied by holding the coverslips with a pair of tweezers in the import/export

buffer (a procedure very useful to achieve really short incubation times), it is possible to save even more money by reducing the amount of radioactivity used for each assay.

During the preparation of this manuscript, a novel procedure for investigating the uptake of AEA in intact cells was reported (51). In this study, Ligresti et al. used TRPV1 channel as a biosensor to detect AEA and developed nanoparticles to deliver AEA into the cytosol, by-passing any interaction with membrane proteins. Using this approach, they found that several agents previously reported to inhibit AEA uptake lose their efficacy when AEA is prevented from interacting with membrane proteins, thus providing novel and more direct evidence for the existence of an AEA transporter (51). Interestingly, because they kept cells in quartz cuvettes or Petri dishes for fluorescence and digital holographic quantitative phase microscopy, respectively, it is tempting to suggest that glass coverslips or chambers could represent a better support also for these novel procedures.

In summary, this study describes a fast, relatively cheap, and reliable glass-based assay for measuring in vitro AEA uptake and release. This approach is aimed at avoiding some of the artifacts generated by the nonspecific binding of AEA to plastic and the complicated kinetics of AEA/BSA interaction. Considering the fact that AEA does not bind appreciably to borosilicate glass, the use of coverslips seems particularly indicated to perform export experiments. More importantly, the new procedure can be also extended to the subcellular level (49, 50) by taking advantage of b-AEA as a nonradioactive probe to look at anandamide trafficking within intact cells by light, fluorescence, and electron microscopy techniques.

The authors gratefully acknowledge Dr. F. Florenzano (Santa Lucia Foundation, Rome, Italy) for helpful discussions.

REFERENCES

1. Devane, W. A., L. Hanus, A. Breuer, R. G. Pertwee, L. A. Stevenson, G. Griffin, D. Gibson, A. Mandelbaum, A. Etinger, and R. Mechoulam. 1992. Isolation and structure of a brain constituent that binds to the cannabinoid receptor. *Science.* **258:** 1946–1949.
2. Van der Stelt, M., and V. Di Marzo. 2005. Anandamide as an intracellular messenger regulating ion channel activity. *Prostaglandins Other Lipid Mediat.* **77:** 111–122.
3. Starowicz, K., S. Nigam, and V. Di Marzo. 2007. Biochemistry and pharmacology of endovanilloids. *Pharmacol. Ther.* **114:** 13–33.
4. Barann, M., G. Molderings, M. Bruss, H. Bonisch, B. W. Urban, and M. Gothert. 2002. Direct inhibition by cannabinoids of human 5–HT3A receptors: probable involvement of an allosteric modulatory site. *Br. J. Pharmacol.* **137:** 589–596.
5. Sawzdargo, M., T. Nguyen, D. K. Lee, K. R. Lynch, R. Cheng, H. H. Heng, S. R. George, and B. F. O'Dowd. 1999. Identification and cloning of three novel human G protein-coupled receptor genes GPR52, PsiGPR53 and GPR55: GPR55 is extensively expressed in human brain. *Brain Res. Mol. Brain Res.* **64:** 193–198.
6. Lauckner, J. E., J. B. Jensen, H. Y. Chen, H. C. Lu, B. Hille, and K. Mackie. 2008. GPR55 is a cannabinoid receptor that increases intracellular calcium and inhibits M current. *Proc. Natl. Acad. Sci. USA.* **105:** 2699–2704.
7. Sun, Y., S. P. Alexander, D. A. Kendall, and A. J. Bennett. 2006. Cannabinoids and PPARalpha signalling. *Biochem. Soc. Trans.* **34:** 1095–1097.
8. Sun, Y., and A. Bennett. 2007. Cannabinoids: a new group of agonists of PPARs. *PPAR Res.* **2007:** 23513.
9. Bouaboula, M., S. Hilairet, J. Marchand, L. Fajas, G. Le Fur, and P. Casellas. 2005. Anandamide induced PPARgamma transcriptional activation and 3T3–L1 preadipocyte differentiation. *Eur. J. Pharmacol.* **517:** 174–181.
10. Gasperi, V., F. Fezza, N. Pasquariello, M. Bari, S. Oddi, A. Finazzi-Agrò, and M. Maccarrone. 2007. Endocannabinoids in adipocytes during differentiation and their role in glucose uptake. *Cell. Mol. Life Sci.* **64:** 219–229.
11. Rockwell, C. E., and N. E. Kaminski. 2004. A cyclooxygenase metabolite of anandamide causes inhibition of interleukin-2 secretion in murine splenocytes. *J. Pharmacol. Exp. Ther.* **311:** 683–690.
12. Cravatt, B. F., K. Demarest, M. P. Patricelli, M. H. Bracey, D. K. Giang, B. R. Martin, and A. H. Lichtman. 2001. Supersensitivity to anandamide and enhanced endogenous cannabinoid signaling in mice lacking fatty acid amide hydrolase. *Proc. Natl. Acad. Sci. USA.* **98:** 9371–9376.
13. Piomelli, D. 2003. The molecular logic of endocannabinoid signalling. *Nat. Rev. Neurosci.* **4:** 873–884.
14. Felder, C. C., A. K. Dickason-Chesterfield, and S. A. Moore. 2006. Cannabinoids biology: the search for new therapeutic targets. *Mol. Interv.* **6:** 149–161.
15. McFarland, M. J., and E. L. Barker. 2004. Anandamide transport. *Pharmacol. Ther.* **104:** 117–135.
16. Dainese, E., S. Oddi, M. Bari, and M. Maccarrone. 2007. Modulation of the endocannabinoid system by lipid rafts. *Curr. Med. Chem.* **14:** 2702–2715.
17. Fowler, C. J., S. Holt, O. Nilsson, K. O. Jonsson, G. Tiger, and S. O. Jacobsson. 2005. The endocannabinoid signaling system: pharmacological and therapeutic aspects. *Pharmacol. Biochem. Behav.* **81:** 248–262.
18. Grotenhermen, F. 2004. Pharmacology of cannabinoids. *Neuroendocrinol. Lett.* **25:** 14–23.
19. Di Marzo, V. 2008. Targeting the endocannabinoid system: to enhance or reduce? *Nat. Rev. Drug Discov.* **7:** 438–455.
20. Centonze, D., A. Finazzi-Agrò, G. Bernardi, and M. Maccarrone. 2007. The endocannabinoid system in targeting inflammatory neurodegenerative diseases. *Trends Pharmacol. Sci.* **28:** 180–187.
21. Maccarrone, M., N. Battista, and D. Centonze. 2007. The endocannabinoid pathway in Huntington's disease: a comparison with other neurodegenerative diseases. *Prog. Neurobiol.* **81:** 349–379.
22. Yates, M. L., and E. L. Barker. 2009. Organized trafficking of anandamide and related lipids. *Vitam. Horm.* **81:** 25–53.
23. Fasia, L., V. Karava, and A. Siafaka-Kapadai. 2003. Uptake and metabolism of [3H]anandamide by rabbit platelets. Lack of transporter? *Eur. J. Biochem.* **270:** 3498–3506.
24. Ortega-Gutierrez, S., E. G. Hawkins, A. Viso, M. L. Lopez-Rodriguez, and B. F. Cravatt. 2004. Comparison of anandamide transport in FAAH wild-type and knockout neurons: evidence for contributions by both FAAH and the CB1 receptor to anandamide uptake. *Biochemistry.* **43:** 8184–8190.
25. Hillard, C. J., W. S. Edgemond, A. Jarrahian, and W. B. Campbell. 1997. Accumulation of N-arachidonoylethanolamine (anandamide) into cerebellar granule cells occurs via facilitated diffusion. *J. Neurochem.* **69:** 631–638.
26. Moore, S. A., G. G. Nomikos, A. K. Dickason-Chesterfield, D. A. Schober, J. M. Schaus, B. P. Ying, Y. C. Xu, L. Phebus, R. M. Simmons, D. Li, et al. 2005. Identification of a high-affinity binding site involved in the transport of endocannabinoids. *Proc. Natl. Acad. Sci. USA.* **102:** 17852–17857.
27. Fegley, D., S. Kathuria, R. Mercier, C. Li, A. Goutopoulos, A. Makriyannis, and D. Piomelli. 2004. Anandamide transport is independent of fatty-acid amide hydrolase activity and is blocked by the hydrolysis-resistant inhibitor AM1172. *Proc. Natl. Acad. Sci. USA.* **101:** 8756–8761.
28. Oddi, S., F. Fezza, N. Pasquariello, C. De Simone, C. Rapino, E. Dainese, A. Finazzi-Agrò, and M. Maccarrone. 2008. Evidence for the intracellular accumulation of anandamide in adiposomes. *Cell. Mol. Life Sci.* **65:** 840–850.
29. McFarland, M. J., A. C. Porter, F. R. Rakhshan, D. S. Rawat, R. A. Gibbs, and E. L. Barker. 2004. A role for caveolae/lipid rafts in the uptake and recycling of the endogenous cannabinoid anandamide. *J. Biol. Chem.* **279:** 41991–41997.
30. Bari, M., N. Battista, F. Fezza, A. Finazzi-Agrò, and M. Maccarrone. 2005. Lipid rafts control signaling of type-1 cannabinoid receptors

in neuronal cells. Implications for anandamide-induced apoptosis. *J. Biol. Chem.* **280:** 12212–12220.
31. Deutsch, D. G., S. T. Glaser, J. M. Howell, J. S. Kunz, R. A. Puffenbarger, C. J. Hillard, and N. Abumrad. 2001. The cellular uptake of anandamide is coupled to its breakdown by fatty-acid amide hydrolase. *J. Biol. Chem.* **276:** 6967–6973.
32. Glaser, S. T., N. A. Abumrad, F. Fatade, M. Kaczocha, K. M. Studholme, and D. G. Deutsch. 2003. Evidence against the presence of an anandamide transporter. *Proc. Natl. Acad. Sci. USA.* **100:** 4269–4274.
33. Kaczocha, M., A. Hermann, S. T. Glaser, I. N. Bojesen, and D. G. Deutsch. 2006. Anandamide uptake is consistent with rate-limited diffusion and is regulated by the degree of its hydrolysis by fatty acid amide hydrolase. *J. Biol. Chem.* **281:** 9066–9075.
34. Fowler, C. J., G. Tiger, A. Ligresti, M. L. Lopez-Rodriguez, and V. Di Marzo. 2004. Selective inhibition of anandamide cellular uptake versus enzymatic hydrolysis–a difficult issue to handle. *Eur. J. Pharmacol.* **492:** 1–11.
35. Karlsson, M., C. Pahlsson, and C. J. Fowler. 2004. Reversible, temperature-dependent, and AM404-inhibitable adsorption of anandamide to cell culture wells as a confounding factor in release experiments. *Eur. J. Pharm. Sci.* **22:** 181–189.
36. Di Marzo, V., A. Fontana, H. Cadas, S. Schinelli, G. Cimino, J. C. Schwartz, and D. Piomelli. 1994. Formation and inactivation of endogenous cannabinoid anandamide in central neurons. *Nature.* **372:** 686–691.
37. Ligresti, A., E. Morera, M. Van Der Stelt, K. Monory, B. Lutz, G. Ortar, and V. Di Marzo. 2004. Further evidence for the existence of a specific process for the membrane transport of anandamide. *Biochem. J.* **380:** 265–272.
38. Palmgren, J. J., J. Monkkonen, T. Korjamo, A. Hassinen, and S. Auriola. 2006. Drug adsorption to plastic containers and retention of drugs in cultured cells under in vitro conditions. *Eur. J. Pharm. Biopharm.* **64:** 369–378.
39. Fezza, F., S. Oddi, M. Di Tommaso, C. De Simone, C. Rapino, N. Pasquariello, E. Dainese, A. Finazzi-Agrò, and M. Maccarrone. 2008. Characterization of biotin-anandamide, a novel tool for the visualization of anandamide accumulation. *J. Lipid Res.* **49:** 1216–1223.
40. Oddi, S., M. Bari, N. Battista, D. Barsacchi, I. Cozzani, and M. Maccarrone. 2005. Confocal microscopy and biochemical analysis reveal spatial and functional separation between anandamide uptake and hydrolysis in human keratinocytes. *Cell. Mol. Life Sci.* **62:** 386–395.
41. Thors, L., and C. J. Fowler. 2006. Is there a temperature-dependent uptake of anandamide into cells? *Br. J. Pharmacol.* **149:** 73–81.
42. Maccarrone, M., M. Di Rienzo, N. Battista, V. Gasperi, P. Guerrieri, A. Rossi, and A. Finazzi-Agrò. 2003. The endocannabinoid system in human keratinocytes. Evidence that anandamide inhibits epidermal differentiation through CB1 receptor-dependent inhibition of protein kinase C, activation protein-1, and transglutaminase. *J. Biol. Chem.* **278:** 33896–33903.
43. Glaser, S. T., M. Kaczocha, and D. G. Deutsch. 2005. Anandamide transport: a critical review. *Life Sci.* **77:** 1584–1604.
44. Battista, N., V. Gasperi, F. Fezza, and M. Maccarrone. 2005. The anandamide membrane transporter and the therapeutic implications of its inhibition. *Therapy.* **2:** 141–150.
45. Rakhshan, F., T. A. Day, R. D. Blakely, and E. L. Barker. 2000. Carrier-mediated uptake of the endogenous cannabinoid anandamide in RBL-2H3 cells. *J. Pharmacol. Exp. Ther.* **292:** 960–967.
46. Fowler, C. J. 2004. Possible involvement of the endocannabinoid system in the actions of three clinically used drugs. *Trends Pharmacol. Sci.* **25:** 59–61.
47. Jonsson, K. O., S. Vandevoorde, D. M. Lambert, G. Tiger, and C. J. Fowler. 2001. Effects of homologues and analogues of palmitoylethanolamide upon the inactivation of the endocannabinoid anandamide. *Br. J. Pharmacol.* **133:** 1263–1275.
48. Maccarrone, M., M. Bari, N. Battista, and A. Finazzi-Agrò. 2002. Estrogen stimulates arachidonoylethanolamide release from human endothelial cells and platelet activation. *Blood.* **100:** 4040–4048.
49. Kaczocha, M., S. T. Glaser, and D. G. Deutsch. 2009. Identification of intracellular carriers for the endocannabinoid anandamide. *Proc. Natl. Acad. Sci. USA.* **106:** 6375–6380.
50. Oddi, S., F. Fezza, N. Pasquariello, A. D'Agostino, G. Catanzaro, C. De Simone, C. Rapino, A. Finazzi-Agrò, and M. Maccarrone. 2009. Molecular identification of albumin and Hsp70 as cytosolic anandamide-binding proteins. *Chem. Biol.* **16:** 624–632.
51. Ligresti, A., L. De Petrocellis, D. Hernan Perez de la Ossa, R. Aberturas, L. Cristino, A. S. Moriello, A. Finizio, M. E. Gil, A. I. Torres, J. Molpeceres, et al. 2010. Exploiting nanotechnologies and TRPV1 channels to investigate the putative anandamide membrane transporter. *PLoS ONE.* **5:** e10239.

ERRATA

An affiliation for Dr. Daniele Piomelli, Italian Institute of Technology, was inadvertently omitted on the following papers Dr. Piomelli co-authored:

Identification of biosynthetic precursors for the endocannabinoid anandamide in the rat brain. *J. Lipid Res.* 2008. 49: 48–57.

Pitfalls and solutions in assaying anandamide transport in cells. *J. Lipid Res.* 2010. 51: 2435–2444.

Plasma lipidomics reveals potential prognostic signatures within a cohort of cystic fibrosis patients. *J. Lipid Res.* 2011. 52: 1011–1022.

The omitted affiliation has now been added to the online versions of these papers.

DOI 10.1194/jlr.M700354-JLR200ERR